

Probing the spin states of three interacting electrons in quantum dots

A. Gamucci,^{1,*} V. Pellegrini,¹ A. Singha,² A. Pinczuk,³ L. N. Pfeiffer,⁴ K. W. West,⁴ and M. Rontani^{5,†}

¹*Istituto Nanoscienze, Consiglio Nazionale delle Ricerche (CNR-NANO) NEST-Pisa and Scuola Normale Superiore, Piazza San Silvestro 12, I-56127 Pisa, Italy*

²*Department of Physics, Bose Institute, 93/1, Acharya Prafulla Chandra Road, Kolkata 700 009, India*

³*Department of Applied Physics and Applied Mathematics and Department of Physics, Columbia University, New York 10027, USA*

⁴*Department of Electrical Engineering, Princeton University, Princeton, and Bell Labs, Alcatel-Lucent, Murray Hill, New Jersey 07974, USA*

⁵*Istituto Nanoscienze, Consiglio Nazionale delle Ricerche (CNR-NANO) S3-Modena, Via Campi 213a, I-41125 Modena, Italy*

(Received 3 October 2011; revised manuscript received 20 December 2011; published 19 January 2012)

We observe a low-lying sharp spin mode of three interacting electrons in an array of nanofabricated AlGaAs/GaAs quantum dots by means of resonant inelastic light scattering. The finding is enabled by a suppression of the inhomogeneous contribution to the excitation spectra obtained by reducing the number of optically probed quantum dots. Supported by configuration-interaction calculations we argue that the observed spin mode offers a direct probe of Stoner ferromagnetism in the simplest case of three interacting spin one-half fermions.

DOI: [10.1103/PhysRevB.85.033307](https://doi.org/10.1103/PhysRevB.85.033307)

PACS number(s): 73.21.La, 73.43.Lp, 73.20.Mf, 31.15.ac

Systems of three charged particles interacting by Coulomb forces are the building blocks of a large variety of correlated quantum phases. An example of current topical interest is represented by the unusual fractional quantum Hall states with nonabelian excitations.^{1,2} On more general grounds, the interaction among at least three particles is essential to account for Stoner ferromagnetism (SF), the paradigm of the tendency of itinerant electrons, such as those responsible for conduction in metals, to align their spins at the expense of their kinetic energy.³

Indeed, the simplest finite-size version of SF displaying the crossover between normal (unpolarized) and spin-polarized degenerate (ferromagnetic) ground states at a threshold interaction strength is offered by three interacting fermions of spin one-half in two dimensions, as: (i) in one dimension the ground state is never spin polarized for any interaction,⁴ and (ii) the two-body ground state is always a spin singlet.⁵ Such a simple system realizes, therefore, a quantum simulator of SF. We recall here that a quantum simulator is a controllable quantum-mechanical device^{6,7} able to tackle difficult quantum many-body problems without the limitations encountered by classical computers when simulating quantum mechanics.

Here we realize and study a solid-state version of the quantum simulator of three interacting fermions based on electrons confined in a semiconductor quantum dot (QD). We show that unpolarized and ferromagnetic states can be probed by monitoring the low-lying neutral spin and charge excitations. We recall that such collective modes in semiconductor QDs can be accessed by resonant inelastic light scattering.^{8–13} We argue that QD systems with three electrons constitute a versatile emulator of the physics of SF.

So far, studies on low-lying neutral spin modes in QDs were performed by optical methods on nanofabricated AlGaAs/GaAs QDs and in self-assembled InAs QDs. In these experiments, however, ensembles of many QDs were investigated owing to the very low signal-to-noise ratio. For example, arrays composed of 10^4 nanofabricated AlGaAs/GaAs QD replicas were studied by us by means of resonant inelastic light scattering.^{9–11,13} In these systems, however, inhomogeneities

in the electron number distribution among the QDs contribute to a significant broadening of the excitation peaks in the detected spectra, leading to a systematic uncertainty in the identification of specific contributions arising from different electron populations. Indeed, the emulation of SF requires access to sharp collective excitations of three electrons that are sufficiently isolated from excitations corresponding to other electron number configurations. This is achieved here in arrays of nanofabricated QDs, which are diluted enough to suppress inhomogeneities linked to number fluctuations. We find that when the number of QD replicas probed in the light scattering experiments is decreased from 10^4 to 10^3 , the inhomogeneities are largely suppressed, leading to a single and sharp spin mode in the excitation spectrum.

We argue in the following that this low-lying mode corresponds to a spin excitation of the three interacting electrons from the ground state with $M = 1$, $S = 1/2$ (M being the total orbital angular momentum and S the total spin of the system) to the excited state with $M = 1$, $S = 3/2$. The assignment is corroborated by accurate full configuration interaction (CI) calculations.^{9,11,13–17} The latter enable linking the measured excitation to the spin-polarized state with $M = 0$, $S = 3/2$ predicted by SF, which is an excited state at the actual value of the electron density.

The three-electron system exhibits a transition to a ferromagnetic state as a function of the Wigner-Seitz parameter r_s , which is the radius of the circle whose area is the average area per electron, in units of the Bohr radius. By knowing both the energy of the transition and the value of the energy spacing $\hbar\omega_0$ among the shells of the potential trap, as retrieved from the measurements, we can thus deduce the energy difference between the absolute ground state of the system and the fully spin-polarized ground state. As it is shown in Fig. 1, this makes it possible to place our results (filled circles in Fig. 1) on a phase diagram showing the path to the realization of SF.

We recall that the essence of SF is summarized by the Stoner criterion.¹⁸ According to that, the ground state is ferromagnetic when $n(E_F)J > 1$, with $n(E_F)$ being the density of states resolved at the Fermi energy and J being proportional to the

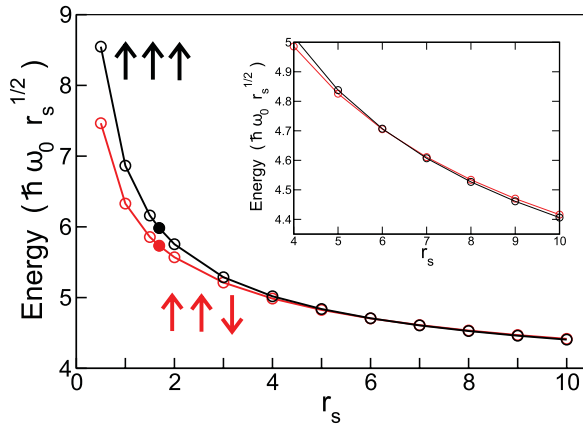


FIG. 1. (Color online) CI energies of the unpolarized (red [gray] circles) and spin-polarized (black circles) three-electron ground states vs r_s . The filled circles point to the values inferred from the inelastic light scattering measurement. Inset: zoom around the crossover. Ten harmonic-oscillator shells were considered in the CI calculation. A square QW of width 25 nm and height 250 meV confines the motion in the out-of-plane direction.

exchange field that splits the energies of electrons of opposite spin. Hence two parameters, namely J and $n(E_F)$, control the relevant physics of the bulk.

The finite-size analog of the criterion, derived in a simple Hartree-Fock picture, is $J/(\hbar\omega_0) > 1$, with $1/(\hbar\omega_0)$ replacing the density of states $n(E_F)$. In our quantum simulator, the first parameter, $\hbar\omega_0$, is obtained through the joint measure of both the electron number N in the QD and the pristine electron density n of the quantum well from which QD arrays are nanofabricated.⁹ For fixed N , $\hbar\omega_0$ is decreased (r_s is increased) by decreasing n . The last parameter, J , is measured from the lowest spin excitation, that is $2\hbar\omega_0 - J$ (cf. inset of Fig. 4).

A series of QD arrays were fabricated on a 25 nm modulation doped GaAs/Al_{0.1}Ga_{0.9}As quantum well (QW) by means of state-of-the-art electron beam lithography and inductively coupled-plasma reactive ion etching. The electron density of the two-dimensional electron gas was $n = 1.1 \times 10^{11} \text{ cm}^{-2}$, and the mobility $2.7 \times 10^6 \text{ cm}^2/\text{Vs}$. Pillars with diameters of 320 nm and aspect ratio of $\sim 2/5$ were produced in 0.1 mm-sized square arrays, in which the number of QD replicas was varied from 10000 down to ≈ 1000 to explore the impact of inhomogeneous broadening on the collective excitations. Resonant inelastic light scattering measurements were performed at $T = 2 \text{ K}$ with a tunable ring-etalon Ti:Sa laser impinging with a spot size of 0.1 mm at normal incidence on the sample. The scattered signal from the QDs was collected by a triple grating spectrometer coupled to liquid N₂-cooled multichannel charge-coupled device (CCD). From previous experiments, it follows that a number of electrons ranging from 2–6 are expected to be confined in such QDs with a confinement energy of $\hbar\omega_0 \approx 4 \text{ meV}$.^{9–11}

We focus first on the sample with 10000 QD replicas. Figure 2(a) shows the results of light scattering measurements of spin density excitations (SDE) obtained with depolarized (perpendicular incident and scattered laser polarizations to detect the spin signal) configuration. Two prominent peaks

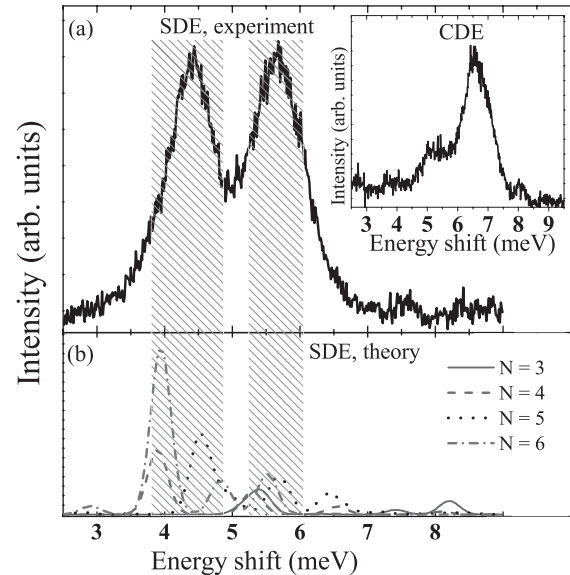


FIG. 2. (a) Experimental spectrum of spin density excitation (SDE) at resonance detected at $T = 2 \text{ K}$ by means of depolarized resonant inelastic light scattering. The inset shows the charge density mode (CDE). (b) CI spectra of SDE obtained for $N = 3, N = 4, N = 5, N = 6$. The shadowed regions are guides to the eye.

emerge in the spin channel at energies of about 4.4 meV and 5.6 meV, respectively, with similar intensities and full width at half maximum (FWHM) of approximately 1 meV. This result matches that of previous experiments in which an average population of four electrons per dot was identified.^{9,11}

In order to single out the contributions due to specific electron populations, we applied the full CI approach to retrieve the theoretical spectra linked to a series of electron populations, ranging from $N = 2$ to $N = 8$, with $\hbar\omega_0$ being fixed by the experimental value of n . This analysis enabled the identification of several prominent contributions to the experimental spectra shown in Fig. 2(a) arising from $N = 3, 4, 5, 6$ electron occupation numbers. Figure 2(b) shows the corresponding calculated spin spectra at resonance. It can be seen that the CI spectral intensities get enhanced as N increases. In addition, while the different contributions overlap with similar intensities in the energy range of the higher-energy peak at around 5.6 meV, the $N = 5$ and $N = 6$ contributions are particularly relevant in the lower-energy range at around 4.5 meV (cf. shadowed areas in Fig. 2). Since the two experimentally detected peaks have similar intensities, it follows that only a very small number of $N = 5$ and $N = 6$ QDs are present in the dense array. Finally there is a single feature associated to the $N = 3$ occupation that appears at around 5.5 meV. Higher-energy peaks resolved in the theoretical simulation are not visible in the experimental spectra probably due to their weaker intensities. For completeness we also show in the inset to Fig. 2(a) the charge density (CDE) spectrum obtained with parallel incident and scattered photon polarizations.

The evolution of the SDE experimental spectra as the number of QDs in the illuminated array is progressively decreased is shown in Fig. 3. These data confirm the interplay between

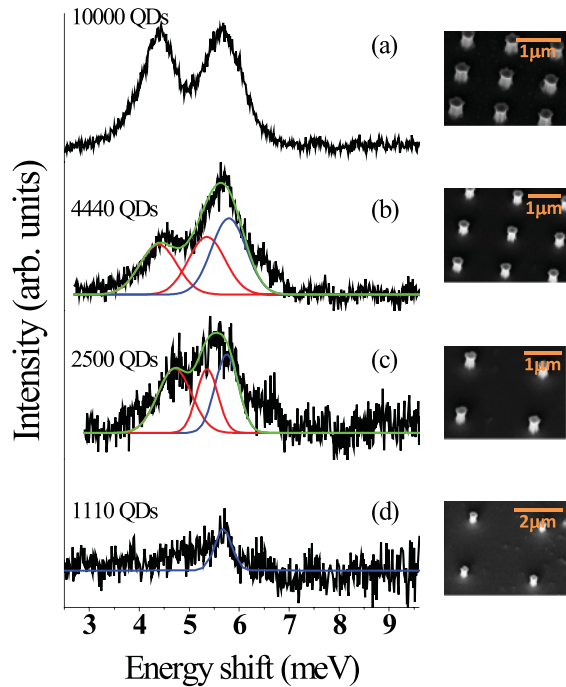


FIG. 3. (Color online) Resonant inelastic light scattering spectra of spin excitations obtained at $T = 2$ K for arrays containing a varying number of QDs. From top to bottom, the number of QDs in the array decreases from 10 000 to 1110 (the interdot distance increases from 1 to $3 \mu\text{m}$). Gaussian fits are superimposed to the experimental spectra in correspondence of three- and four-electron contributions (blue [dark grey] and red [gray] curves, respectively). The resulting global fit is shown as a green [light gray] curve on each spectrum. On the right-hand side, a scanning electron microscope image of the studied QDs is shown, in correspondence to each case.

the different electron populations allowing the isolation of the specific contribution of the QDs with three interacting electrons. There is a significant reduction of the intensity of the lower-energy peak as we reduce the number of QDs from 10 000 to 4440. We attribute it to the vanishing contributions of the $N = 5$ and $N = 6$ occupations in the more dilute array. As we further reduce the QD density, the relative intensities of the two peaks are driven by the interplay between the $N = 4$ and $N = 3$ electron occupations. At the lowest QD density of 1100, the contribution of $N = 4$ to the lower-energy peak is barely visible, indicating that the number of QDs with $N = 4$ is close to the threshold value for optical detection. This, together with the reduction of the peak linewidths due to the lower impact of inhomogeneous broadening allows us to ascribe the well-defined peak in the 1100-QD array spectrum to QDs with $N = 3$.

In Figs. 3(b), 3(c), and 3(d), Gaussian fits centered at Raman energies matching with the CI predictions [Fig. 2(b)] have been considered in order to globally reproduce the experimental data. It follows that: (i) the two slightly shifted peaks relative to $N = 3$ (blue [dark grey] curve in Fig. 3) and $N = 4$ (red [gray] curve) present at ~ 5.6 meV broaden the overall parent structure (green [light gray] curve) to ~ 1 meV FWHM for the 4440-QD array [Fig. 3(b)], and (ii) the progressive narrowing of the peaks due to the vanishing of the $N = 4$ feature in

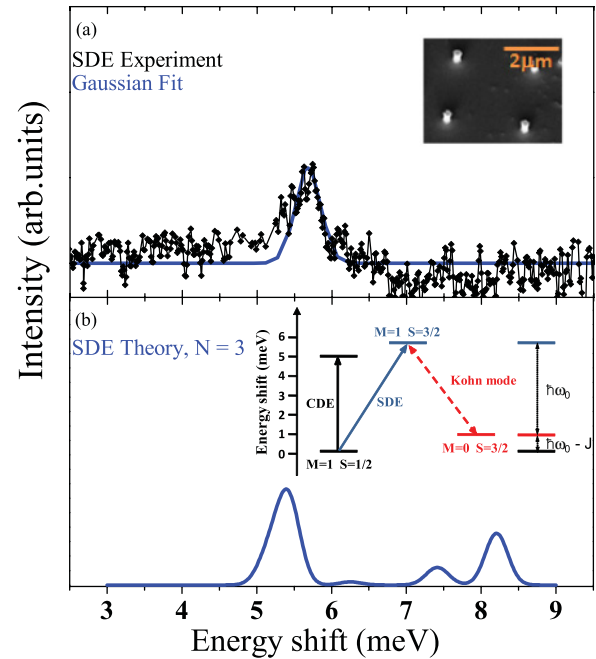


FIG. 4. (Color online) (a) Experimental resonant inelastic light scattering spectrum (black curve with points) and Gaussian fit (continuous blue [dark grey] curve) for the spin channel for the 1110-QD array. A scanning electron microscope image of the relative QD array is also shown. (b) Configuration-interaction calculations of spin density excitation for $N = 3$. The inset shows the energy diagram of relevant transitions.

the less dense arrays makes the linewidth of the high-energy peak decrease down to the limiting value of 0.4 meV FWHM for 1110 QDs [blue (dark grey) curve in Fig. 3(d)]. We thus eventually managed to realize a system in which only the population of three electrons is present. The spectrum of the spin excitation measured for the array of 1110 QDs is reproduced in Fig. 4 together with the pertinent CI prediction for $N = 3$.

By comparing the top and bottom panels of Figs. 4 and 3, it emerges that the $N = 3$ contribution has been identified and selected out of a more complex background. The lowness of the signal, at the limit of the signal-to-noise detection threshold, implies that only the most intense peak, centered at ~ 5.5 meV, can be safely identified.

The transition energies involved in the measurement are indicated in the inset to Fig. 4. The retrieved monopole SDE links the ground state, characterized by $M = 1$ and $S = 1/2$, to an excited state with $M = 1$, $S = 3/2$. The final state of this transition is also accessible via a Kohn mode excitation from the ferromagnetic ground state with $M = 0$, $S = 3/2$. Remarkably, the two spin-polarized states with $M = 0$ and $M = 1$ differ only in the center-of-mass motion, whose excitation—exactly of energy $\hbar\omega_0$ —is insensitive to interactions. Therefore, with regard to the nontrivial part of the wave function that is affected by interactions, the final state of the observed SDE is a replica of the ferromagnetic ground state. This attribution is crucial to address the realization of a spin-polarized state relevant to the study of Stoner ferromagnetism.

Finally we remark that cold Fermi atoms confined in optical traps have been proposed as finite-size simulators of three-body interaction phenomena¹⁹ and SF physics. They are simple systems able to drive SF through the tunable short-range atom-atom interaction.^{20–22} However, this capability is limited by the losses due to three-body recombination.

In conclusion, we have identified the low-lying modes of three interacting electrons in a quantum dot by means of inelastic light scattering. By decreasing the number of optically probed QDs we were able to suppress the inhomogeneities related to the simultaneous presence of different electron populations leading to a spin excitation spectrum dominated by a single and sharp (FWHM of 0.4 meV) peak. By a detailed comparison with calculations based on a configuration interaction method we have linked the observed peak to a transition from the $M = 1, S = 1/2$ ground state to the $M = 1, S = 3/2$ excited state of the three interacting electrons. The

results presented in this Brief Report mark a starting point for the simulation of Stoner ferromagnetism in a solid-state system composed by three electrons confined in a semiconductor quantum dot and for the investigation of the competition between spin-unpolarized $S = 1/2$ and spin-polarized $S = 3/2$ states.

We thank G. Goldoni and E. Molinari for stimulating discussions. This work is supported by Ministero dell'Istruzione, dell'Università e della Ricerca with project PRIN Grant No. 2008H9ZAZR, Fondazione Cassa di Risparmio di Modena with project "COLDandFEW", and CINECA-ISCRA project Grant No. HP10BIFGH8. A. Pinczuk was supported by NSF under Grant No. DMR-0803445 and by the Nanoscale Science and Engineering Initiative of NSF under Grant No. CHE-0641523.

*andrea.gamucci@nano.cnr.it

†massimo.rontani@nano.cnr.it

¹G. Moore and N. Read, *Nucl. Phys. B* **360**, 362 (1991).

²A. Wojs, C. Toke, and J. K. Jain, *Phys. Rev. Lett.* **105**, 196801 (2010).

³E. C. Stoner, *Proceedings of the Royal Society of London, series A* **165**, 372 (1938).

⁴E. Lieb and D. Mattis, *Phys. Rev.* **125**, 164 (1962).

⁵D. C. Mattis, *The Theory of Magnetism* (Harper, New York, 1965).

⁶I. Buluta and F. Nori, *Science* **326**, 108 (2009).

⁷A. Singha *et al.*, *Science* **332**, 1176 (2011).

⁸T. Brocke, M.-T. Bootsman, M. Tews, B. Wunsch, D. Pfannkuche, Ch. Heyn, W. Hansen, D. Heitmann, and C. Schüller, *Phys. Rev. Lett.* **91**, 257401 (2003).

⁹C. P. Garcia, V. Pellegrini, A. Pinczuk, M. Rontani, G. Goldoni, E. Molinari, B. S. Dennis, L. N. Pfeiffer, and K. W. West, *Phys. Rev. Lett.* **95**, 266806 (2005).

¹⁰S. Kalliakos, C. P. Garcia, V. Pellegrini, M. Zamfirescu, L. Cavigli, M. Gurioli, A. Vinattieri, A. Pinczuk, B. S. Dennis, L. N. Pfeiffer, and K. W. West, *Appl. Phys. Lett.* **90**, 181902 (2007).

¹¹S. Kalliakos, M. Rontani, V. Pellegrini, C. P. Garcia, A. Pinczuk, G. Goldoni, E. Molinari, L. N. Pfeiffer, and K. W. West, *Nat. Phys.* **4**, 467 (2008).

¹²T. Köppen, D. Franz, A. Schramm, Ch. Heyn, D. Heitmann, and T. Kipp, *Phys. Rev. Lett.* **103**, 037402 (2009).

¹³A. Singha, V. Pellegrini, A. Pinczuk, L. N. Pfeiffer, K. W. West, and M. Rontani, *Phys. Rev. Lett.* **104**, 246802 (2010).

¹⁴S. M. Reimann and M. Manninen, *Rev. Mod. Phys.* **74**, 1283 (2002).

¹⁵M. Rontani, S. Amaha, K. Muraki, F. Manghi, E. Molinari, S. Tarucha, and D. G. Austing, *Phys. Rev. B* **69**, 085327 (2004).

¹⁶M. Rontani and E. Molinari, *Phys. Rev. B* **71**, 233106 (2005).

¹⁷M. Rontani, C. Cavazzoni, D. Bellucci, and G. Goldoni, *J. Chem. Phys.* **124**, 124102 (2006).

¹⁸G. Grosso and G. Pastori Parravicini, *Solid State Physics* (Academic Press, San Diego, 2000).

¹⁹H. P. Büchler, A. Micheli, and P. Zoller, *Nature Physics* **3**, 726 (2007).

²⁰R. A. Duine and A. H. MacDonald, *Phys. Rev. Lett.* **95**, 230403 (2005).

²¹G.-B. Jo, Y.-R. Lee, J.-H. Choi, C. A. Christensen, T. H. Kim, J. H. Thywissen, D. E. Pritchard, and W. Ketterle, *Science* **325**, 1521 (2009).

²²X.-J. Liu, H. Hu, and P. D. Drummond, *Phys. Rev. A* **82**, 023619 (2010).